

**This is a self-archived version of an original article. This version may differ from the original in pagination and typographic details.**

**Author(s):** Lewis, M.C.; Joss, D.T.; Sayđı, B.; Page, R.D.; Cullen, D.M.; Barber, L.; Giles, M.M.; Simpson, J.; Al-Aqeel, M.A.M.; Badran, H.; Braunroth, T.; Briscoe, A.D.; Calverley, T.; Dewald, A.; Doncel, M.; Grahn, T.; Greenlees, P.T.; Henrich, C.; Herzáň, A.; Herzberg, R.-D.; Higgins, E.; Hilton, J.; Ilieva, S.; Julin, R.; Juutinen, S.; Keatings, J.; Kröll, T.; Labiche, M.; Mashtakov, K.; Nara Singh, B.S.; Parr, E.; Partanen, J.; Paul,

**Title:** Lifetime measurements of excited states in  $^{163}\text{W}$  and the implications for the anomalous  $B(E2)$  ratios in transitional nuclei

**Year:** 2019

**Version:** Published version

**Copyright:** © 2019 The Authors.

**Rights:** CC BY 4.0

**Rights url:** <https://creativecommons.org/licenses/by/4.0/>

**Please cite the original version:**

Lewis, M.C., Joss, D.T., Sayđı, B., Page, R.D., Cullen, D.M., Barber, L., Giles, M.M., Simpson, J., Al-Aqeel, M.A.M., Badran, H., Braunroth, T., Briscoe, A.D., Calverley, T., Dewald, A., Doncel, M., Grahn, T., Greenlees, P.T., Henrich, C., Herzáň, A., . . . Uusitalo, J. (2019). Lifetime measurements of excited states in  $^{163}\text{W}$  and the implications for the anomalous  $B(E2)$  ratios in transitional nuclei. *Physics Letters B*, 798, Article 134998-  
<https://doi.org/10.1016/j.physletb.2019.134998>



# Lifetime measurements of excited states in $^{163}\text{W}$ and the implications for the anomalous $B(E2)$ ratios in transitional nuclei

M.C. Lewis<sup>a</sup>, D.T. Joss<sup>a,\*</sup>, B. Saygı<sup>b</sup>, R.D. Page<sup>a</sup>, D.M. Cullen<sup>c</sup>, L. Barber<sup>c</sup>, M.M. Giles<sup>c</sup>, J. Simpson<sup>d</sup>, M.A.M. Al-Aqeel<sup>a,e</sup>, H. Badran<sup>f</sup>, T. Braunroth<sup>g</sup>, A.D. Briscoe<sup>a</sup>, T. Calverley<sup>a,f</sup>, A. Dewald<sup>g</sup>, M. Doncel<sup>a</sup>, T. Grahn<sup>f</sup>, P.T. Greenlees<sup>f</sup>, C. Henrich<sup>h</sup>, A. Herzán<sup>a,i</sup>, R.-D. Herzberg<sup>a</sup>, E. Higgins<sup>a</sup>, J. Hilton<sup>a,f</sup>, S. Ilieva<sup>h</sup>, R. Julin<sup>f</sup>, S. Juutinen<sup>f</sup>, J. Keatings<sup>j</sup>, T. Kröll<sup>h</sup>, M. Labiche<sup>d</sup>, K. Mashtakov<sup>j</sup>, B.S. Nara Singh<sup>c,j</sup>, E. Parr<sup>a</sup>, J. Partanen<sup>f</sup>, E.S. Paul<sup>a</sup>, P. Rahkila<sup>f</sup>, M. Sandzelius<sup>f</sup>, J. Sarén<sup>f</sup>, C. Scholey<sup>f</sup>, M. Siciliano<sup>k,l</sup>, P. Spagnoletti<sup>j</sup>, S. Stolze<sup>f</sup>, S.V. Szewc<sup>f</sup>, M.J. Taylor<sup>m</sup>, J. Uusitalo<sup>f</sup>

<sup>a</sup> Department of Physics, Oliver Lodge Laboratory, University of Liverpool, Liverpool L69 7ZE, United Kingdom

<sup>b</sup> Fizik Bölümü, Fen Fakültesi, Ege Üniversitesi, Bornova, İzmir, 35100, Turkey

<sup>c</sup> School of Physics & Astronomy, Schuster Building, The University of Manchester, Manchester M13 9PL, United Kingdom

<sup>d</sup> UKRI-STFC Daresbury Laboratory, Daresbury, Warrington WA4 4AD, United Kingdom

<sup>e</sup> Imam Mohammad Ibn Saud Islamic University (IMISU), Riyadh, 11623, Saudi Arabia

<sup>f</sup> Department of Physics, University of Jyväskylä, Department of Physics, P.O. Box 35, FI-40014, Jyväskylä, Finland

<sup>g</sup> Institut für Kernphysik der Universität zu Köln, Zùlpicher Strasse 77, D-50937 Köln, Germany

<sup>h</sup> Institut für Kernphysik, TU Darmstadt, Schlossgartenstr. 9, 64289 Darmstadt, Germany

<sup>i</sup> Institute of Physics, Slovak Academy of Sciences, SK-84511 Bratislava, Slovakia

<sup>j</sup> School of Engineering & Computing, University of the West of Scotland, Paisley, United Kingdom

<sup>k</sup> INFN, Laboratori Nazionali di Legnaro, 35020 Legnaro (Padova), Italy

<sup>l</sup> Ifju/CEA, Université de Paris-Saclay, 91191 Gif-sur-Yvette, France

<sup>m</sup> Division of Cancer Sciences, School of Medical Sciences, The University of Manchester, Manchester, M13 9PL, United Kingdom

## ARTICLE INFO

### Article history:

Received 28 June 2019

Accepted 2 October 2019

Available online 7 October 2019

Editor: D.F. Geesaman

### Keywords:

Mean lifetimes

$B(E2)$  reduced transition probabilities

Recoil-distance Doppler-shift method

Nuclear deformation

Gamma-ray Spectroscopy

## ABSTRACT

This letter reports lifetime measurements of excited states in the odd- $N$  nucleus  $^{163}\text{W}$  using the recoil-distance Doppler shift method to probe the core polarising effect of the  $i_{13/2}$  neutron orbital on the underlying soft triaxial even-even core. The ratio  $B(E2:21/2^+ \rightarrow 17/2^+)/B(E2:17/2^+ \rightarrow 13/2^+)$  is consistent with the predictions of the collective rotational model. The deduced  $B(E2)$  values provide insights into the validity of collective model predictions for heavy transitional nuclei and a geometric origin for the anomalous  $B(E2)$  ratios observed in nearby even-even nuclei is proposed.

© 2019 The Authors. Published by Elsevier B.V. This is an open access article under the CC BY license (<http://creativecommons.org/licenses/by/4.0/>). Funded by SCOAP<sup>3</sup>.

## 1. Introduction

The emergence of collective phenomena in atomic nuclei is a central paradigm in many-body quantum physics. The residual interactions between the increasing number of valence protons and neutrons outside closed shells result in low-energy configurations with deformed shapes. The onset of deformation promotes a ge-

ometry in which one or more axes of rotation become distinct from the nuclear symmetry axis and collective rotational excitations begin to dominate the spectrum of states at low angular momenta [1]. The low-lying excited states in the heavy neutron-deficient nuclei above  $N = 82$  reflect the evolution from non-collective excitations in spherical nuclei near the closed shell to collective rotational bands in well-deformed axial rotors near the midshell.

The low-lying levels vary smoothly between these two regimes through a transitional region characterised by soft triaxial shapes,

\* Corresponding author.

E-mail address: david.joss@liverpool.ac.uk (D.T. Joss).

see for example [2]. A more definitive understanding of collectivity can be obtained from the measurement of  $B(E2)$  reduced transition probabilities. In heavy neutron-deficient nuclei, considerable progress has been made through measurements of excited-state lifetimes using Doppler shift methods in conjunction with selective decay correlation techniques [3]. The relationship between level excitation energies and  $B(E2: 2^+ \rightarrow 0^+)$  values in the Os [4], W [5] and Pt [6] nuclei with the number of valence nucleons is readily interpreted in terms of collective models. However, ratios of reduced transition probabilities for some even-even transitional nuclides are much lower than expected from the predictions of the rotational model [4–7]. This letter reports the results of lifetime measurements of excited states in the transitional nucleus,  $^{163}\text{W}$ . The deduced  $B(E2)$  values constrain expectations of collective model predictions for heavy transitional nuclei and suggest a geometric origin for the anomalous  $B(E2)$  ratios observed in nearby even-even nuclei.

## 2. Experimental details

Excited states in  $^{163}\text{W}$  were populated via the  $^{106}\text{Cd}(^{60}\text{Ni}, 2pn)^{163}\text{W}$  fusion-evaporation reaction in an experiment performed at the University of Jyväskylä Accelerator Laboratory, Finland. The  $^{60}\text{Ni}$  beam bombarded a self-supporting isotopically enriched  $^{106}\text{Cd}$  target foil of thickness  $1.1 \text{ mg/cm}^2$  with a Ta support of thickness  $1.3 \text{ mg/cm}^2$ . The Ta foil was placed facing the beam resulting in a bombarding energy of 270 MeV and an initial reaction fragment velocity of  $v/c=3.1\%$  at the front of the  $^{106}\text{Cd}$  target. The target was stretched and mounted in the DPUNS differential plunger device [8] along with a downstream  $1.0 \text{ mg/cm}^2$  Mg degrader, which resulted in a reduction in recoil velocity of fusion-evaporation residues to  $v/c=2.1\%$ . The target-to-degrader distance,  $x$ , was changed to allow excited-state lifetimes to be measured using the recoil-distance Doppler-shift (RDDS) technique [3]. Gamma rays emitted at the target position were detected by the JUROGAM II  $\gamma$ -ray spectrometer comprising 15 Eurogam Phase 1-type [9] and 24 Eurogam clover [10] escape-suppressed hyperpure germanium detectors.

The velocity-degraded fusion-evaporation residues were transported through the RITU gas-filled separator [11,12] and implanted into the double-sided silicon strip detectors (DSSDs) of the GREAT spectrometer located at the focal plane [13]. A planar double-sided germanium strip detector was mounted behind the DSSDs inside the same vacuum enclosure to detect X rays and low-energy  $\gamma$  rays [13]. Three clover Ge detectors were mounted perpendicular to the DSSDs outside the vacuum chamber to detect higher-energy  $\gamma$  rays. All detector signals were timestamped to a precision of 10 nanoseconds by the total data readout data acquisition system [14]. Gamma rays detected at the target and focal-plane positions in delayed coincidence with the implanted recoils were analysed offline with the GRAIN data-analysis package [15].

## 3. Results

Excited states in  $^{163}\text{W}$  were measured in several prior experiments and bands associated with single-quasineutron  $f_{7/2}$ ,  $h_{9/2}$ , and  $i_{13/2}$  configurations have been observed [16–18]. A partial level scheme for  $^{163}\text{W}$  is displayed in Fig. 1 illustrating  $\gamma$ -ray transitions in the  $\nu i_{13/2}$  band and its decay paths to the  $7/2^-$  ground state. In the present study, the lifetimes of the yrast  $17/2^+$  and  $21/2^+$  states in  $^{163}\text{W}$  were measured using the recoil-distance Doppler-shift method [3]. The experiment used 11 different target-to-degrader distances ranging from 30 to 5000  $\mu\text{m}$ . The Phase 1-type detectors used in this analysis were positioned at  $158^\circ$  (5 detectors) and  $134^\circ$  (10 detectors) relative to the beam direction,

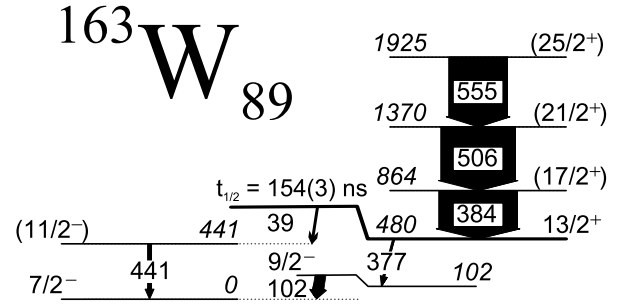


Fig. 1. Partial level scheme showing levels and transitions in the yrast band of  $^{163}\text{W}$  and its decay paths to the  $7/2^-$  ground state [16,17]. The levels are labelled by their spins, parities, and excitation energies. All energies are stated in keV. The half-life of the  $13/2^+$  isomer is taken from reference [17].

which allowed the Doppler-shifted and degraded components of  $\gamma$ -ray transitions to be identified. Lifetimes were extracted using the Differential Decay Curve Method (DDCM) [19], of which two variations were used: a recoil-correlated  $\gamma$ -ray coincidence analysis and an isomer-tagged singles analysis.

The recoil-correlated  $\gamma$ -ray coincidence analysis has the advantage of eliminating side feeding to the level of interest. For each distance measured,  $\gamma$  rays in delayed coincidence with recoil implantations in the DSSDs were sorted into two separate asymmetric two-dimensional matrices; one consisting of  $\gamma$  rays detected at  $158^\circ$  versus coincident  $\gamma$  rays detected either at  $158^\circ$  or  $134^\circ$  and the other consisting of  $\gamma$  rays detected at  $134^\circ$  versus coincident  $\gamma$  rays detected either at  $158^\circ$  or  $134^\circ$ . Gamma-ray coincidences with the fully shifted component of the  $555 \text{ keV } 25/2^+ \rightarrow 21/2^+$  transition were projected onto the  $\theta = 134^\circ$  or  $158^\circ$  axes of their respective matrices. Typical spectra generated using this method are shown in Fig. 2.

These data were analysed using the DDCM for  $\gamma$ -ray coincidences [19,20]. For coincidences demanded with the fully Doppler shifted component ( $s$ ) of an indirect feeding transition  $C$  (with corresponding degraded component  $d$ ), a level with feeding transition  $B$  and depopulating transition  $A$  has a lifetime given by

$$\tau(x) = \frac{\{C_s, A_d\}(x) - \alpha\{C_s, B_d\}(x)}{\frac{d}{dx}\{C_s, A_s\}(x)} \cdot \frac{1}{v}, \quad (1)$$

where quantities in braces are coincident intensities at target-to-degrader distance  $x$ ,  $v$  is the average recoil velocity and  $\alpha = (\alpha(x))_x$  with

$$\alpha(x) = \frac{\{C_s, A_d\}(x) + \{C_s, A_s\}(x)}{\{C_s, B_d\}(x) + \{C_s, B_s\}(x)}, \quad (2)$$

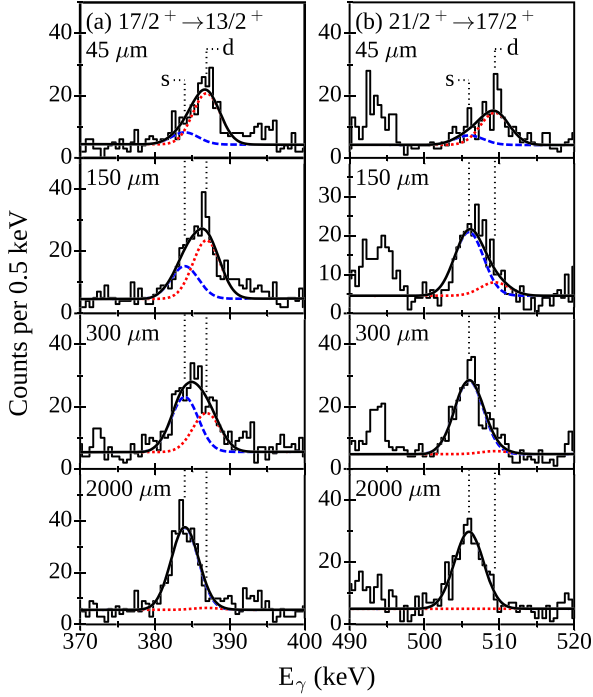
which corrects for differences in measured intensities in the depopulating and feeding transitions.

Fig. 3 shows the decay curves and lifetimes determined using normalised intensities extracted from the coincidence spectra. The mean lifetime was obtained by a weighted average of the values at each distance within the region of sensitivity.

The  $13/2^+$  band head is isomeric with a half-life of  $154(3) \text{ ns}$  and is depopulated via two distinct  $\gamma$ -ray cascades to the ground state [17]. These isomer-delayed  $\gamma$  rays may be detected in the GREAT planar and clover detectors at the RITU focal plane and can be used as a selective tag for  $\gamma$ -ray emissions at the target position. The  $555 \text{ keV}$   $\gamma$ -ray transition that is used to select the  $\nu i_{13/2}$  band in  $^{163}\text{W}$  in the recoil-correlated  $\gamma$ -ray coincidence analysis is overlapped by the intense  $552 \text{ keV}$  transition originating from  $^{164}\text{W}$  [21], which is a strongly populated exit channel in this reaction. An isomer-decay tagged singles analysis was performed in order to confirm that this contamination in the selecting transition

**Table 1**  
Measured lifetimes and reduced transition probabilities for excited states in  $^{163}\text{W}$ .

$E_\gamma$ (keV)	$I_i^\pi \rightarrow I_f^\pi$ (h)	Detector angle	Recoil-correlated $\gamma$ -ray coincidences	Isomer-tagged singles	Average values	
			$\tau$ (ps)	$\tau$ (ps)	$\tau$ (ps)	$B(E2)_\downarrow$ (W.u.)
384.1	$17/2^+ \rightarrow 13/2^+$	158°	21.3(30)		22(2)	80(8)
		134°	21.4(30)			
		134°		26.5(50)		
506.2	$21/2^+ \rightarrow 17/2^+$	158°	2.3(6)		3.0(4)	154(23)
		134°	3.8(7)			



**Fig. 2.** Recoil-correlated  $\gamma\gamma$  spectra measured at  $\theta = 134^\circ$  to the beam axis for (a) the 384 keV transition depopulating and (b) the 506 keV transition feeding the  $17/2^+$  state. Coincidences were demanded with the fully Doppler-shifted component of the 555 keV transition detected at the  $\theta = 134^\circ$  or  $158^\circ$  positions for all spectra shown. Fits for the fully Doppler-shifted (s) and degraded (d) components are shown by the blue dashed and red dotted lines, respectively, while the total is shown by the black solid line.

does not significantly affect the measured lifetime. Recoiling  $^{163}\text{W}$  nuclei were selected on the condition that implantations were followed within  $0.5 \mu\text{s}$  by a 102, 377 or 441 keV  $\gamma$  ray detected in the planar Ge detector or a 377 or 441 keV  $\gamma$  ray detected in the clover Ge detectors at the RITU focal plane.

In a singles analysis, for a level  $i$  fed by levels  $h$  and feeding the level  $j$ , the lifetimes of excited states are given by

$$\tau(x) = - \frac{Q_{ij}(x) - b_{ij} \sum_h (J_{hi}/J_{ij}) Q_{hi}(x)}{\frac{d}{dx} Q_{ij}(x)} \cdot \frac{1}{v}. \quad (3)$$

Here  $Q_{ij}(x) = I_{ij}^d(x)/(I_{ij}^s(x) + I_{ij}^d(x))$  and  $I_{ij}^d(x)$  and  $I_{ij}^s(x)$  are the  $\gamma$ -ray intensities for the degraded and shifted components, respectively,  $b_{ij}$  is the branching ratio of level  $i$  and  $J_{hi}$ ,  $J_{ij}$  are the relative intensities of respective transitions [19]. In this analysis, the assumption was made that the unobserved feeding of the  $17/2^+$  levels has the same time dependence as that of the observed feeding.

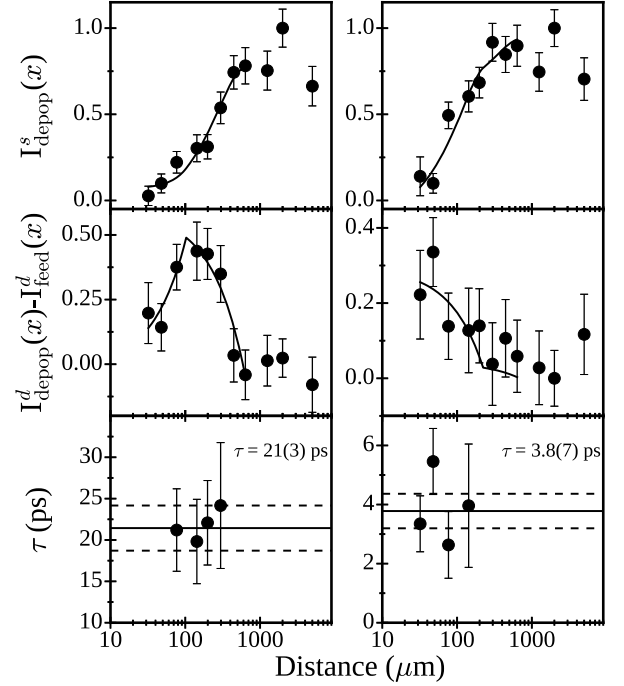


**Fig. 3.** DDCM analysis for the  $17/2^+$  (left) and  $21/2^+$  (right) levels. Top: normalised fully shifted intensity of the depopulating transition measured at  $\theta = 134^\circ$ . Middle: difference in intensity between the degraded components of the depopulating and feeding transitions. Bottom: lifetimes measured at distances within the region of sensitivity. The solid line indicates the weighted average while the dashed lines are the error bars.

The weighted averages of the lifetimes measured using the coincidence and singles analyses are shown in Table 1 along with the corresponding  $B(E2)$  values, which were calculated using the relation

$$B(E2; I_i \rightarrow I_f) = \frac{0.0816}{E_\gamma^5 (1 + \alpha) \tau}, \quad (4)$$

where  $I_i$  and  $I_f$  are the spins of the initial and final levels, respectively,  $E_\gamma$  is the  $\gamma$ -ray energy of the transition in MeV,  $\alpha$  is the internal conversion coefficient for the transition [22] and  $\tau$  is the mean lifetime in ps of the emitting state.

#### 4. Discussion

Fig. 4(a) compares the  $B(E2: 17/2^+ \rightarrow 13/2^+)$  values measured in the odd- $A$  W isotopes with the  $B(E2: 2^+ \rightarrow 0^+)$  values in the even- $A$  isotopes as a function of neutron number. The  $B(E2)$  values vary as a function of neutron number with lower values observed in the transitional isotopes above the  $N = 82$  closed shell and higher values in the deformed midshell region. The  $B(E2)$  values

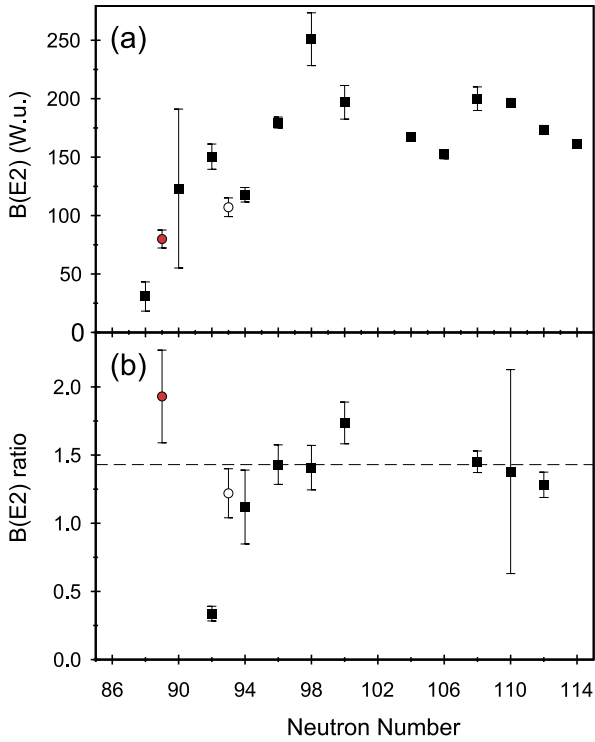


**Fig. 4.** (a)  $B(E2: 17/2^+ \rightarrow 13/2^+)$  values for odd- $N$  (circles) and  $B(E2: 2^+ \rightarrow 0^+)$  for even- $N$  W isotopes (filled squares). (b) Ratios of  $B(E2)$  values for W isotopes. The ratio is  $B(E2: 21/2^+ \rightarrow 17/2^+)/B(E2: 17/2^+ \rightarrow 13/2^+)$  for odd- $N$  isotopes and  $B(E2: 4^+ \rightarrow 2^+)/B(E2: 2^+ \rightarrow 0^+)$  for even- $N$  isotopes. The dashed line is the ratio predicted by the collective rotational model for even- $N$  isotopes. The measurements for  $^{163}\text{W}$  are indicated by red circles. Data are taken from refs. [23,31–41].

for the measured odd- $A$  W isotopes follow the general trend established by the  $B(E2: 2^+ \rightarrow 0^+)$  values. This pattern is consistent with the expectations of nuclear models [23].

The ratios of reduced transition probabilities in  $^{166}\text{W}$  and other heavy neutron-deficient nuclei have apparently anomalous values that cannot be reproduced in terms of the collective rotational model [4–7]. This is illustrated in Fig. 4(b) which compares the  $B(E2: 4^+ \rightarrow 2^+)/B(E2: 2^+ \rightarrow 0^+)$  with the predictions of the collective model [24]. Similarly low ratios are observed in several mass regions of the nuclear chart [25–29].

The even- $A$   $N \geq 94$  W isotopes have ratios that are consistent with the theoretical ratio of 1.43. However, the isotope  $^{166}\text{W}$  is an excellent example where several excited-state lifetimes have been measured but anomalous  $B(E2)$  ratios have been extracted. The  $B(E2: 4^+ \rightarrow 2^+)/B(E2: 2^+ \rightarrow 0^+)$  ratio is significantly lower than the theoretical prediction at 0.33(5) [5]. It has been proposed that the W-Os-Pt nuclei undergo a phase transition between non-collective seniority and collective excitations [6]. In nuclei that have low average ground-state deformations such a transition between non-collective low-spin states and collective high-spin states can occur [30]. However, in nuclei such as  $^{166}\text{W}$  where the  $B(E2: 2^+ \rightarrow 0^+)$  values are in excess of 100 W.u. alternative mechanisms must be considered.

In this region, a common feature of even- $A$  nuclei with apparently anomalous  $B(E2)$  ratios is that they have ratios of  $4^+$  to  $2^+$  excitation energies close to that of a gamma-soft rotor [ $E(4^+)/E(2^+) \approx 2.5$ ]. Soft-triaxial nuclear deformations arise due to the spatial density distributions for protons and neutrons at the top and bottom of their shells, respectively or vice versa [42]. In the  $N \sim 92$  nuclei,  $\gamma$ -soft shapes arise from the competing polarising effects of protons in the high- $\Omega$   $h_{11/2}$  orbitals and neutrons in the low- $\Omega$   $f_{7/2}$ ,  $h_{9/2}$  and  $i_{13/2}$  orbitals, where  $\Omega$  is the projec-

tion of the single-particle angular momentum on the symmetry axis. This is reflected in the ratio of  $4^+$  to  $2^+$  excitation energies in the ground-state bands of neutron-deficient W isotopes, which have values close to the  $\gamma$ -soft limit of  $E(4^+)/E(2^+) = 2.5$ . The  $E(4^+)/E(2^+)$  ratios for  $^{162}\text{W}$  [21],  $^{164}\text{W}$  [21] and  $^{166}\text{W}$  [43] are 2.25, 2.48 and 2.68, respectively. Furthermore, the signature splitting between the low-spin states of coupled bands in the neighbouring odd- $Z$  isotones is also indicative of  $\gamma$ -soft triaxial shapes [44–46]. A parallel study has measured the lifetimes of low-lying states in  $^{163}\text{Ta}$  to confirm its quadrupole and triaxial deformations [47].

The wavefunctions of nuclear states are sensitive to the geometric shapes adopted by nuclei [48]. The  $B(E2)$  values calculated in the rotational model depend on the projections of single-particle angular momenta on the symmetry axis. The projection of the total angular momentum on the symmetry axis ( $K$ ) is a good quantum number for axially deformed nuclei with a unique rotation axis but is ill-defined for soft-triaxial shapes. Therefore, the measured properties of triaxial nuclei may deviate from the predictions of collective rotational models that assume axial symmetry and hence a well-defined  $K$ -value. It follows that the resulting  $B(E2)$  ratios in odd- $A$  W isotopes should be consistent with the collective model if the odd neutron occupies an orbital that polarises the soft-triaxial core towards an axial prolate shape. The angular momentum of the single- $i_{13/2}$  neutron is directed in a quasi-parallel direction to the core angular momentum and has a small component along the symmetry axis. Thus, the  $i_{13/2}$  neutron is expected to have a strong polarising effect on the core due to its spatial orientation in an equatorial orbit. Indeed, the core-polarising influence of the  $i_{13/2}$  neutron configurations is apparent in the three-quasiparticle structures of the light Ta isotopes, which are formed by coupling a single  $h_{11/2}$  proton to neutron configurations in their underlying W cores [44].

In this work, lifetimes have been measured from both the  $17/2^+$  and  $21/2^+$  states in the  $\nu i_{13/2}$  band of  $^{163}\text{W}$ . Fig. 4(b) compares the present measurements of ratios of reduced transition probabilities with those of the heavier isotopes including  $^{167}\text{W}$ , which is currently the only other transitional odd- $A$  isotope for which lifetime measurements have been performed [41]. High- $j$  and low- $\Omega$  orbitals in odd- $A$  nuclei are highly susceptible to the Coriolis force and are effectively decoupled from the core rotation [49]. In such cases, the spectrum of excited states is characterised by rotational excitations of the even-even core coupled to angular momentum of the decoupled neutron. For this reason, the  $B(E2: 21/2^+ \rightarrow 17/2^+)/B(E2: 17/2^+ \rightarrow 13/2^+)$  ratios extracted for odd- $N$  isotopes are compared with the theoretical value of 1.43 predicted for the even-even isotopes. A ratio of  $B(E2: 21/2^+ \rightarrow 17/2^+)/B(E2: 17/2^+ \rightarrow 13/2^+) = 1.93(34)$  was measured for the isotope  $^{163}\text{W}$ , which is within  $2\sigma$  of the theoretical value predicted by the rotational model. The ratio extracted for  $^{167}\text{W}$  using the measurements of Li et al. is similarly close to the axial limit. These measurements suggest that there is no anomaly in either  $^{167}\text{W}$  or  $^{163}\text{W}$  whose core is expected to be closer to the  $\gamma$ -soft limit.

These results indicate that rotational collective models are applicable in transitional odd- $A$  nuclei when the occupation of a rotationally aligned high angular momentum orbital restores axial symmetry to an otherwise soft-triaxial even-even core. The anomalous  $B(E2)$  ratios observed in even- $A$  nuclei are attributed to soft-triaxial shapes that result in poorly defined  $K$  quantum numbers and perturbed rotational wavefunctions.

## 5. Summary

The mean lifetimes of the  $17/2^+$  and  $21/2^+$  states in the  $\nu i_{13/2}$  band of  $^{163}\text{W}$  have been measured using the recoil-distance Doppler-Shift method in an experiment using the JUROGAM II  $\gamma$ -ray spectrometer in conjunction with the DPUNS differential plunger device. The ratio of extracted  $B(E2)$  reduced transition probabilities is found to be consistent with the predictions of the collective rotational model. This agreement within experimental ( $2\sigma$ ) uncertainties suggests that the  $\nu i_{13/2}$  configuration of  $^{163}\text{W}$  adopts an axial prolate shape. This is a marked difference from the  $B(E2)$  ratios extracted for the nearby even-even nuclei such as  $^{166}\text{W}$ . The anomalous  $B(E2)$  ratios in  $^{166}\text{W}$  and other nearby transitional nuclei are therefore attributed to their  $\gamma$ -soft triaxial shapes for which  $K$  is poorly defined with consequences for nuclear wavefunctions and their dependent  $B(E2)$  values. This hypothesis could provide a useful test for the predictions of fully self-consistent mean field models that do not rely on the assumptions made in collective or geometric models.

## Acknowledgements

This work has been supported by the UK Science and Technology Facilities Council under grants ST/P004598/1, ST/L005670/1 and ST/L005794/1; the Scientific and Technological Research Council of Turkey (TUBITAK Project No: 117F508); the EU HORIZON2020 programme “Infrastructures”, project number: 654002 (ENSAR2) and by the Academy of Finland under the Finnish Centre of Excellence Programme (Nuclear and Accelerator Based Physics Programme at JYFL). The UK/France (STFC/IN2P3) Loan Pool and GAMMAPOOL network are acknowledged for the HPGe escape-suppressed detectors of the JUROGAM II array.

## References

- [1] A. Bohr, B.R. Mottelson, *Nuclear Structure Volume 2: Nuclear Deformation*, W. A. Benjamin Inc., New York, USA, 1975.
- [2] Qiong Yang, Hua-Lei Wang, Min-Liang Liu, Fu-Rong Xu, *Phys. Rev. C* 94 (2016) 024310.
- [3] A. Dewald, O. Möller, P. Petkov, *Prog. Part. Nucl. Phys.* 67 (2012) 786.
- [4] T. Grahn, et al., *Phys. Rev. C* 96 (2016) 044327.
- [5] B. Saygi, et al., *Phys. Rev. C* 96 (2017) 021301(R).
- [6] B. Cederwall, et al., *Phys. Rev. Lett.* 121 (2018) 022502.
- [7] R.B. Cakirli, R.F. Casten, J. Jolie, N. Warr, *Phys. Rev. C* 70 (2004) 047302.
- [8] M.J. Taylor, et al., *Nucl. Instrum. Methods Phys. Res., Sect. A* 707 (2013) 143–148.
- [9] C.W. Beausang, et al., *Nucl. Instrum. Methods Phys. Res., Sect. A* 313 (1992) 37.
- [10] G. Duchene, et al., *Nucl. Instrum. Methods Phys. Res., Sect. A* 432 (1999) 90.
- [11] J. Uusitalo, et al., *Nucl. Instrum. Methods Phys. Res. B* 204 (2003) 638.
- [12] J. Saren, J. Uusitalo, M. Leino, J. Sorri, *Nucl. Instrum. Methods Phys. Res. A* 654 (2011) 508.
- [13] R.D. Page, et al., *Nucl. Instrum. Methods Phys. Res. B* 204 (2003) 634.
- [14] I.H. Lazarus, et al., *IEEE Trans. Nucl. Sci.* 48 (2001) 567.
- [15] P. Rauhkila, *Nucl. Instrum. Methods Phys. Res., Sect. A* 595 (2008) 637–642.
- [16] J. Thomson, et al., *Phys. Rev. C* 81 (2010) 014307.
- [17] C. Scholey, et al., *Phys. Rev. C* 81 (2010) 014306.
- [18] G.D. Dracoulis, et al., *Proceedings of the International Conference of Nuclear Structure at High Angular Momentum, Ottawa, AECL Report No. vol. 2* (1992) 94 (unpublished).
- [19] A. Dewald, et al., *Z. Phys. A* 334 (1989) 163.
- [20] G. Böhm, A. Dewald, P. Petkov, P. von Brentano, *Nucl. Instrum. Methods Phys. Res., Sect. A* 329 (1993) 248.
- [21] D.T. Joss, et al., *Phys. Rev. C* 93 (2016) 024307.
- [22] T. Kibédi, T.W. Burrows, M.B. Trzhaskovskaya, P.M. Davidson, C.W. Nestor Jr., *Nucl. Instrum. Methods Phys. Res., Sect. A* 589 (1992) 202.
- [23] M. Doncel, et al., *Phys. Rev. C* 95 (2017) 044321.
- [24] D.J. Rowe, J.L. Wood, *Fundamentals of Nuclear Models: Foundational Models, vol. 1*, World Scientific, 2009.
- [25] D. Hertz-Kintish, L. Zamick, S.J.Q. Robinson, *Phys. Rev. C* 90 (2014) 034307.
- [26] M.M. Giles, et al., *Phys. Rev. C* 99 (2019) 044317.
- [27] C. Louchart, et al., *Phys. Rev. C* 87 (2013) 0543902.
- [28] G. de Angelis, et al., *Phys. Lett. B* 535 (2002) 93–102.
- [29] O. Möller, et al., *Phys. Rev. C* 71 (2005) 064324.
- [30] J.J. Ressler, et al., *Phys. Rev. C* 69 (2004) 034317.
- [31] C.M. Baglin, *Nucl. Data Sheets* 111 (2010) 1807.
- [32] C.M. Baglin, E.A. McCutchan, S. Basunia, *Nucl. Data Sheets* 153 (2018) 1.
- [33] B. Singh, *Nucl. Data Sheets* 75 (1995) 199.
- [34] E. Browne, Huo Junde, *Nucl. Data Sheets* 87 (1999) 15.
- [35] J.M. Regis, et al., *Nucl. Instrum. Methods Phys. Res., Sect. A* 606 (2009) 466.
- [36] M. Rudigier, et al., *Nucl. Phys. A* 847 (2010) 89.
- [37] E.A. McCutchan, *Nucl. Data Sheets* 126 (2015) 151.
- [38] B. Singh, *Nucl. Data Sheets* 130 (2015) 21.
- [39] C.M. Baglin, *Nucl. Data Sheets* 111 (2010) 275.
- [40] C.M. Baglin, *Nucl. Data Sheets* 99 (2003) 1.
- [41] C.B. Li, et al., *Phys. Rev. C* 94 (2016) 044307.
- [42] Y.S. Chen, S. Frauendorf, G.A. Leander, *Phys. Rev. C* 28 (1983) 2437.
- [43] J. Simpson, et al., *J. Phys. G* 18 (1992) 1207.
- [44] K. Lagergren, et al., *Phys. Rev. C* 83 (2011) 014313.
- [45] M. Sandzelius, et al., *Phys. Rev. C* 80 (2009) 054316.
- [46] T.R. Davis-Merry, et al., *Phys. Rev. C* 91 (2015) 034319.
- [47] L. Barber, et al., (2019), submitted for publication.
- [48] G. Alaga, K. Alder, A. Bohr, B.R. Mottelson, *Dan. Mat. Fys. Medd.* 29 (1955) 1.
- [49] F.S. Stephens, *Rev. Mod. Phys.* 29 (1975) 43.